Extraterrestrial mining via two coupled thermal-driven phenomena

Jesus A. Dominguez[1],
Insight Global/Jacobs Space Exploration Group (JSEG), Huntsville, AL, 35806

Brittany Brown[2], Kagen Crawford[3], Paul Hintze[4], Cara Black[5], Ellen Rabenberg[6]
NASA Marshall Space Flight Center, Huntsville, Alabama, 35811

Shannon McCall[7]
Qualis Corporation /Jacobs Space Exploration Group (JSEG), Huntsville, AL, 35806

Two-coupled thermal-driven phenomena, Marangoni effect and thermal fractional decomposition under high vacuum, previously observed by the authors could lead to an extraterrestrial mining operation that would significantly reduce mechanical operation and allow in-situ product extraction directly from the mineral without the necessity of neither mineral beneficiation nor use of terrestrial precursors. Thermal Marangoni effect alone and coupled with fractional decomposition have been corroborated through paths of 10 and 13 inches respectively on molten JSC-1A lunar regolith simulant presenting a novel and valuable potential for extraterrestrial mining as the observed outcome (self-transportation via Marangoni effect and fractional decomposition at higher temperature) will be more prominent on extraterrestrial surfaces under higher vacuum and reduced gravity. A comprehensive 3D model built by the authors demonstrated to be a crucial tool to determine the right location of the sample to optimize the gradient temperature along the wall of a long tubular crucible enhancing the Marangoni effect as surface tension (the driving force for the thermal Marangoni effect) depends on the temperature gradient.

Nomenclature

Al	=	aluminum
AMU	=	Atomic Molecular Unit
CO_2	=	carbon dioxide
Fe	=	Iron
ISRU	=	in-situ resources utilization
MSFC	=	Marshall Space Flight Center
NASA	=	National Aeronautics and Space Administration
N_2	=	nitrogen
O_2	=	oxygen
ISS	=	International Space Station
JSC	=	Johnson Space Center
RGA	=	Residual Gas Analyzer
SEM	=	scanning electron microscope
Si	=	silicon
Ti	=	Titanium
THVC	=	Thermal High-Vacuum Chamber
W	=	tungsten

[1] ECLSS Principal Investigator, MSFC ECLSS Development Branch, Mail Stop: ES62, MSFC, AL 35812.
[2] ECLSS Engineer, MSFC ECLSS Development Branch, Mail Stop: ES62, MSFC, AL 35812.
[3] Chemical Engineer, MSFC ECLSS Development Branch, Mail Stop: ES62, MSFC, AL 35812.
[4] Branch Chief, MSFC ECLSS Development Branch, Mail Stop: ES62, MSFC, AL 35812.
[5] Acting Deputy Branch Chief, MSFC ECLSS Development Branch, Mail Stop: ES62, MSFC, AL 35812.
[6] Material Engineer, MSFC Failure Analysis and Metallurgy Branch, Mail Stop: EM31, MSFC, AL 35812.
[7] Senior Mechanical Engineer, MSFC ECLSS Development Branch, Mail Stop: ES62, MSFC, AL 35812.

I. Introduction

The Marangoni effect is frequently observed while drinking wine with 12% or larger ethanol contains as a ring of wine formed near the top of the glass generates droplets that fall back into the wine. In this phenomenon, known as Tears of wine, the Marangoni effect is driven by the surface tension created via gradient on ethanol concentration and temperature along the three-phase, liquid wine, solid wall, and gas air. Besides being observed while drinking wine, the Marangoni effect is crucial for welding metals, manufacturing integrated circuits, and growing crystals. This paper aims to establish that thermal Marangoni effect coupled with material decomposition under the high vacuum conditions at the moon and asteroids have the potential to be crucial supporting extraterrestrial mining and other interplanetary endeavors, as vacuum and reduced gravity are expected to augment the Marangoni effect on extraterrestrial molten soil leading to sustainable extraterrestrial in-situ resources utilization (ISRU).

Previous Marangoni effect assessment on molten lunar regolith via JSC-1A lunar regolith simulant under vacuum generated a spontaneous upwards migration of a uniform molten thin-film front as well as at bulk scale that climbed the crucible wall covering the entire wall's surface and reaching the crucible's top end[1]. Further assessment on higher-temperature vacuum-driven decomposition of the uniform thin-film front as it climbed the crucible's wall revealed a significant decomposition of various simulant's metal-oxide components into their respective oxygen and metal elements strengthening the feasibility of extraterrestrial generation and fractional separation of oxygen and metals/alloys with none or minimal need for terrestrial precursors. These two coupled phenomena, thermal Marangoni effect and fractional decomposition, will be more prominent on extraterrestrial surfaces under much higher vacuum and reduced gravity opening novel pathways in extraterrestrial mining and manufacturing

The Thermal Marangoni effect alone and coupled with fractional decomposition of metal oxides, further segregation of the decomposed components, and oxygen (O_2) release were observed on molten JSC-1A lunar regolith simulant by the authors at Marshall Space Flight Center (MSFC) and reported in this paper. The upwards migration paths observed and reported in this paper, 10 and 13 inches respectively, are longer than those reported previosly[1] validating further the potential utilization of these two coupled phenomena in extraterrestrial mining. Segregation of several decomposed components observed and reported here was neither observed previously[1].

Decomposition and release of O_2 were confirmed by direct measurement of O_2 via a 100 Atomic Molecular Unit (AMU) Residual Gas Analyzer (RGA) installed on the downstream of the vacuum line outlet; SEM/EDX analysis was conducted on the melt samples removed at different positions in the upwards migration path to quantify the composition of the melt and corroborate not only fractional decomposition but also further segregation.

The test stand designed and built by the authors can operate at temperatures as high as 1,600 Celsius and house longer and wider tubular crucibles to carry larger samples with lengthier upwards migration paths. A comprehensive 3D model built by the authors demonstrated to be a crucial tool to determine the optimal location of the tubular crucible to obtain the largest temperature gradient along the crucible's wall to boost the thermal Marangoni effect.

Future extraterrestrial mining will require an operational approach completely different from the terrestrial one that heavily relies on not only mechanical excavation and transportation but also on a stand-alone refinery process to extract the mineral components. In this paper, the authors propose an extraterrestrial all-in-one mining process in which the Marangoni effect would allow non-mechanical transportation of the extraterrestrial mineral to feed an also in-situ pyrolysis-based refinery unit.

II. Marangoni Effect

The Marangoni effect[2] leads to the motion of liquids through a three-phase junction driven by surface tension gradients generated by changes in composition and temperature, the main two variables that govern surface tension. A surface tension gradient induced by local variations in composition is called solutal Marangoni effect[3]. Surface tension gradients induced by changes in temperature are usually known as thermocapillary flow[4], or thermal Marangoni effect. In tears of wine[5], a classical example of solutal Marangoni effect, a meniscus is formed at the three-phase junction between the wine glass walls, wine, and air then the liquid in the meniscus loosely clings to the surface of the glass. The meniscus is formed because the walls of the glass have a hydrophilic surface. Wine contains ethanol that evaporates faster in the meniscus than in the flat bulk flat surface due to the meniscus higher surface area in relation to its small volume. Therefore, it generates an ethanol concentration gradient between the meniscus and the flat bulk causing a surface tension gradient that moves the meniscus up the walls of the glass. As the meniscus gets more depleted of alcohol, which in turn causes a larger surface tension gradient, more wine gets pulled up the walls of the glass until droplets form. Gravity takes effect and tears of wine run down the sides of the glass and back into the flat bulk of the wine.

Thermal-driven Marangoni effect under vacuum causing upwards migration of oil caused by a temperature gradient along the wall was reported by Tazioukov[6]. Experiments using different vacuum working fluids on metallic surfaces, often used in vacuum technology, were used to prove the theoretical results. The results obtained provide a better understanding of the surface migration process due to the temperature gradient and allow for control of the oil film displacement. Kundan[7] found that temperature gradients near the heated end of a wickless heat pipe in microgravity might be high enough to generate a thermal Marangoni effect and lead thermocapillary forces that resist the return flow of liquid from the cold end. The experiments were conducted at the International Space Station (ISS) using a transparent heat pipe combination to generate images and thermal data.

III. Test Stand

A vertical-tubular Thermal High-Vacuum Chamber (THVC) has been designed and built to conduct the study and characterization of both thermal-driven phenomena on molten extraterrestrial simulant samples, upwards migration and fractional decomposition that are the fundamentals of the experimental work. Figure 1 illustrates a schematic (not at scale) of the THVC that basically consists of (1) one meter long, 110-mm ID, 100-mm OD alumina tube, (2) a 508-mm long, 52-mm OD, 45-mm ID one-end-closed alumina tube housing the simulant sample and hanging from the top SS flange, and 3) a top viewport equipped with a blue-laser (465-nm wavelength) illumination system aimed to witness/record the upward migration of the molten sample throughout the inner wall of the sample holder tube. The sample holder is long enough (508 mm) to allow the molten sample to extensively migrate upwards and concurrently decomposes into metals, alloys and oxygen driven by the fact that the high vacuum present within the THVC allows the sample components to decompose into their elements at lower temperature. Two SS flanges are positioned at both ends of the main alumina tube, the top SS flange is equipped with three ports, one is connected to the vacuum line, the second one holds the viewport that allows the investigators to witness/record the thermal-driven migration, and the third one is connected to the Residual Gas Analyzer (RGA that measures gaseous O_2, water vapor, nitrogen (N_2), carbon dioxide (CO_2), and up to 100 Atomic-Molecular-Unit (AMU) gases. Two different vacuum setup approaches are available to attempt reaching the highest vacuum level; in the first approach two diffusion vacuum pumps are coupled to the top and bottom sides of alumina tube and both connected with a scroll pump as illustrated in Figure 1. In the second approach, the bottom diffusion pump is eliminated while the top diffusion pump is replaced with a turbo pump. SiC heater elements in direct contact with the main alumina tube provides the heat source for the THVC. An insulation layer wraps the heating elements and the main alumina tube providing the required insulation along the heating zone. The one-end-closed tube housing the sample is loaded on to the top of the main alumina tube by hanging it from the top SS flange using two hooks.

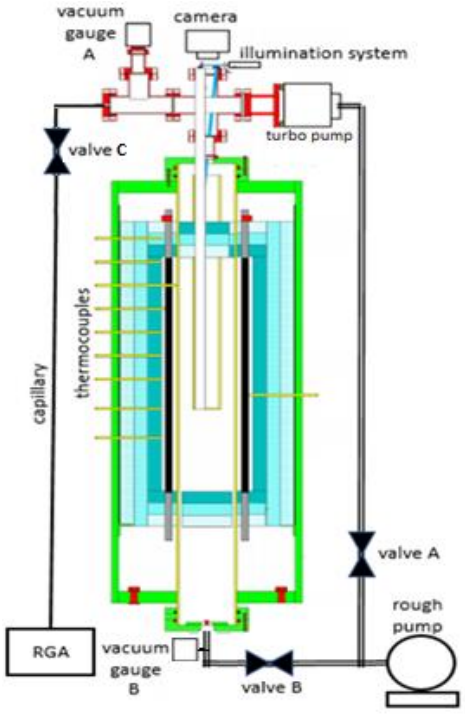

Figure 1. General THVC schematic

The THVC is equipped with a single resistively heating zone intended to operate at temperatures on the order of 1,500 Celsius and 10^{-6} torr. The heating elements consisting of sixteen silicon carbide (SiC) rods are evenly spaced forming a hot wall around the alumina tube. The alumina tube is sealed on both ends through silicone O-rings, insulated by a set of concentric insulating tubes and blankets. Stable, programmable temperature control capability is provided by a process controller system.

Key THVC's process performance specifications include:

Work Volume: 100 mm diameter, approximately 20" long.
Operating Temperature: 1,600 Celsius Maximum
Maximum Ramp Rates: 20 Celsius per minute
Forced cooling Rate: Process tube gas flow can cool sample
Operating Atmosphere: Vacuum down to 10^{-6} torr inside alumina tube.

The THVC's equipment specifications include:

Process Chamber: Alumina Tube, 1 meter long/110mm ID/100 mm OD Nominal

Hot Zone Assembly: Sixteen 27”-long SiC elements surrounded by insulation.
Vacuum System: One turbo pump connected to the top side of the alumina tube and one rough pump connected to the turbo pump and the bottom side of the alumina tube.
Illumination system: A 1.5W blue (450 nm) laser module installed on top of a viewport to allow illumination inside the ceramic tube.

Figure 2 depicts three different views of the THVC’s test stand designed and built in-house at NASA Marshall Flight Center. In Figure 2a key elements can be identified, such as the RGA, vacuum controller, blue laser illumination system and camera, HVTC, vacuum gauge, diffusion and turbo pumps; in Figure 2b the sample loading side is identified; Figure 2b depicts two monitor screens displaying the RGA plot and the image of the melt sample illuminated with a blue-laser emitter and acquired by the camera installed on the top.

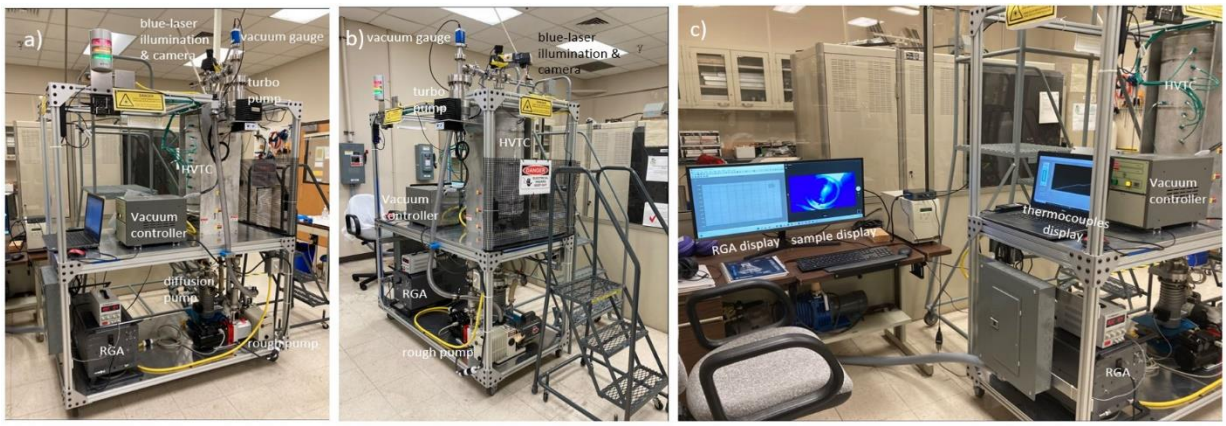

Figure 2. Three different views of the THVC’s test stand designed and built in-house at MSFC.

The test stand is mainly equipped with a vertical alumina tube (3.25-inch OD, 3.0-inch ID, and 40-inch length), a high vacuum system (turbo-rough on the top and diffusion-rough on the bottom), sixteen Silicon Carbide (SiC) heating rods, top/bottom inner insulation, a heating controller, eight thermocouples, a camera mounted on a viewport illuminated with a blue-laser emitter, and an RGA.

IV. 3D model

A comprehensive 3D THVC‘s model was built to estimate the optimal location of the tubular crucible hanging from the top flange and housing the sample and attain the largest temperature gradient along the tube’s wall as the driving force of the thermal Marangoni effect is the temperature gradient along the crucible wall. The 3D model is at scale, includes all the THVC’s elements, and has a comprehensive approach as heat fluxes derived from surface-to-surface thermal radiation and free convection flow are rigorously estimated.

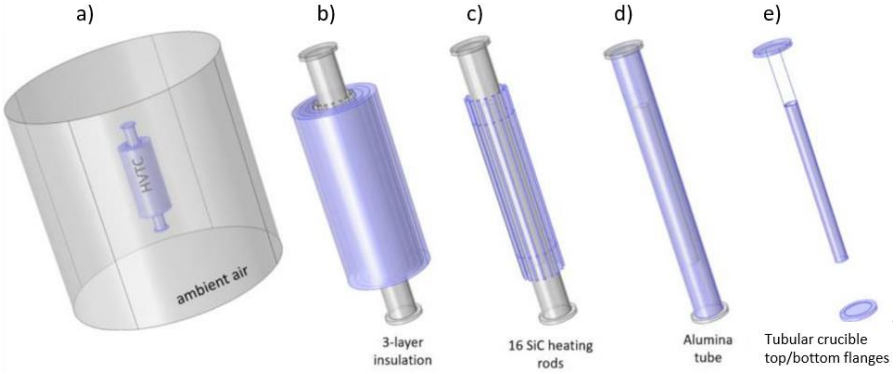

Figure 3. Material domains used in the comprehensive 3D model. a) ambient air, b) 3-layer insulation, c) 16 SiC heating rods, d) alumina tube, e) tubular crucible.

Figure 3 shows the key model's domains: a) the ambient-air domain wrapping the THVC's domain large enough, compared with the HTVC's domain size, to fairly assume that air temperature on the outer surface is ambient getting higher as air approaches the THVC domain generating heat transfer between both domains and triggering natural thermal-driven convective air flow, b) the three insulation layers, c) the sixteen SiC heating rods around the alumina tube, d) the alumina tube, and e) the tubular crucible (one-end-closed tube) housing the sample and hanging from the top flange.

Figure 4 shows some outcomes of the comprehensive 3D THVC's model built to determine the optimal location of the tubular crucible housing the sample to obtain the largest temperature gradient along the tube's wall and boost thermal Marangoni effect. The temperature profile on the air surrounding the THVC as well as the temperature profile on the THVC are shown in Figure 4a. The thermal radiosity profile generated inside the THVC by the 16 SiC heating rods is shown in Figure 4b, Temperature profiles on the inner section of the THVC and tubular crucible are shown in Figure c.

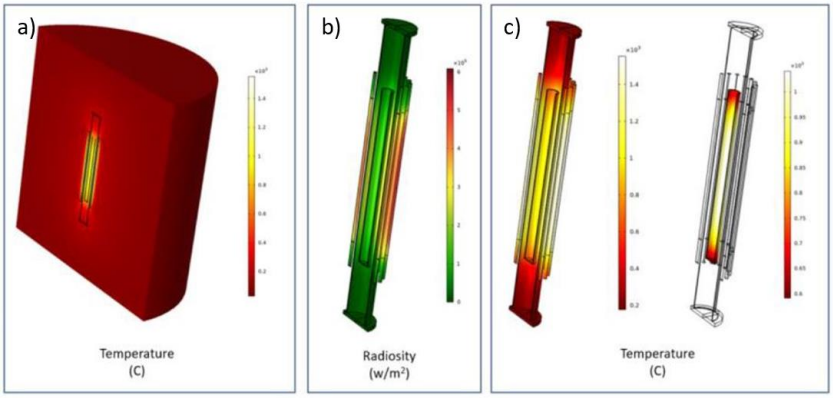

Figure 4. Outcomes of the comprehensive 3D THVC's. a) Temperature profile on air and THVC, b) Thermal radiosity within the THVC, c) Temperature within the THVC, and d) Temperature within tubular crucible housing the sample.

V. Experimental Outcome

150 grams of JSC-1A lunar regolith samples were housed in a tubular crucible having 2.0-inch OD, 1.75-inch ID, and 16-inch length. The 150 grams of simulant occupied 1.25 inches of the 16-inch wall length leaving 14.75 inches of bared inner wall. At 1,300 Celsius and 3.7E-3 torr of vacuum the melt did not decompose as the RGA did not detect any O_2 and elemental oxygen (O) peaks but it formed a meniscus on the surface in contact with the crucible's wall and uniformly migrated upwards climbing 13 of the 14.75 inches of originally bared wall. At 1,400 Celsius and 1.2E-3 torr of vacuum the melt's metal oxides mildly decomposed as the RGA registered small peaks of O_2 and O and also formed a meniscus on the melt's surface in contact with the crucible's wall that led to not only shorter upwards migration than previously observed (10 instead of 13 inches) but also different coloration (brown instead of black) and texture (mostly shiny on the bottom section with dendritic spots instead of speckled shiny surfaces without

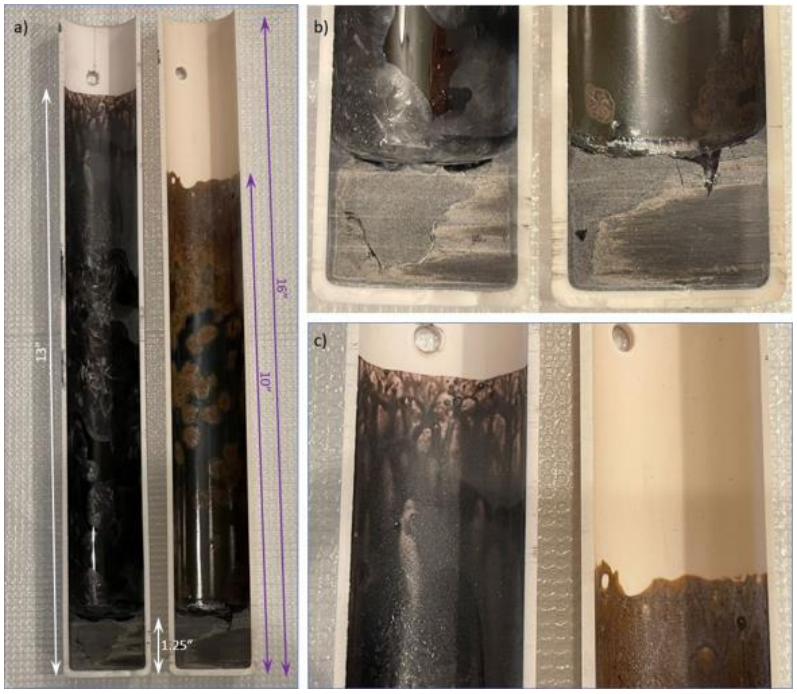

Figure 5. a) Interior of two tubular crucibles housing the same amount (150 grams) of JSC-1A lunar regolith simulant melts generated at 1,300 (3.7E-3 torr) and 1,400 C (1.2E-3 torr) cases respectively, b) Magnified section of the meniscus formed in both cases, c) front end of the upwards migration in both cases.

dendritic spots). Figure 5 summarizes the outcome on these two cases, Figure 5a depicts the interior of two tubular crucibles housing the same amount (150 grams) of JSC-1A melts generated in both cases. Figure 5b depicts a magnified section of the meniscus formed in both cases on the surface of the melt in contact with the crucible's wall. Figure 5c depicts the front end of the upwards migration in both cases, a ring of clear melt, near the top of the front end, is formed and from which streaks dropped back into the melt.

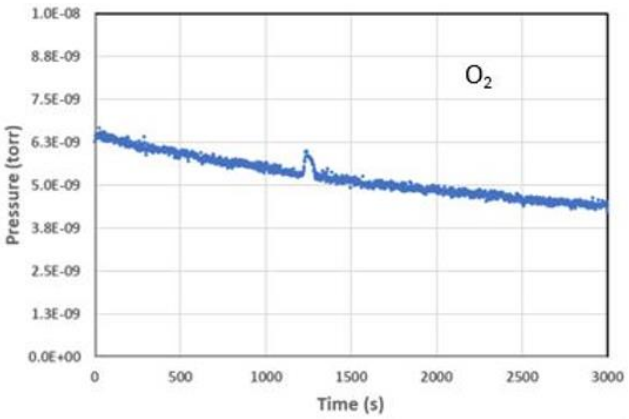

Figure 6. O_2 partial pressure peaks detected by the RGA at 1,400 C and 1.2E-3 torr vacuum.

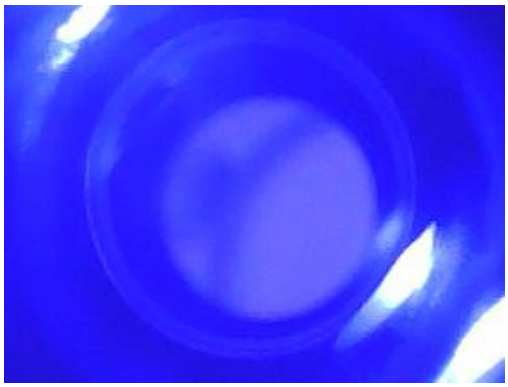

Figure 7. Image of the melt taken by the camera mounted on the top of the HVTC under blue-laser illumination at 1,400 C

Figure 6 shows O_2 partial pressure peak detected and measured by the RGA at 1,300 Celsius and 3.7E-3 torr (right tubular crucible in Figure 5a); partial pressures of O_2 and atomic O gradually decreases with temperature as oxygen as O_2 and O (O_2 and vapor water) degas yielding a peak if a source of O_2/O different than degassing releases O_2 or vapor water. The peak detected and shown in Figure 6 might be due to the decomposition of some metal oxides originally in the melt. Figure 7 depicts the image of the melt at 1,400 C under blue-laser illumination taken by the camera mounted on the top of the THVC.

The tubular crucibles were cut vertically in half as shown in Figure 5 and samples from three different positions (bottom, middle, and top) along the tubular crucible wall were extracted to determine their composition via scanning electron microscope (SEM) and energy dispersive X-ray (EDX) spectroscopy. Figure 8 shows the six samples (three per crucible) and the respective extraction locations within the crucibles. Samples 1, 2, and 3 were extracted from the bottom, middle, and top respectively of the tubular crucible exposed to 1,300 Celsius and 3.7E-3 torr; samples 4, 5, and 6 were extracted from the bottom, middle, and top respectively of the tubular crucible exposed to 1,400 Celsius and 1.2E-3 torr. Sample 6 had many rust-colored features while sample 5 had some of the rust-colored features, but also had a smooth black color. Sample 3 did not appear to have a large amount of the rust-colored features but was very textured. Samples 1, 2, and 4 were mainly smooth with some mild texturing/surface features on the surface.

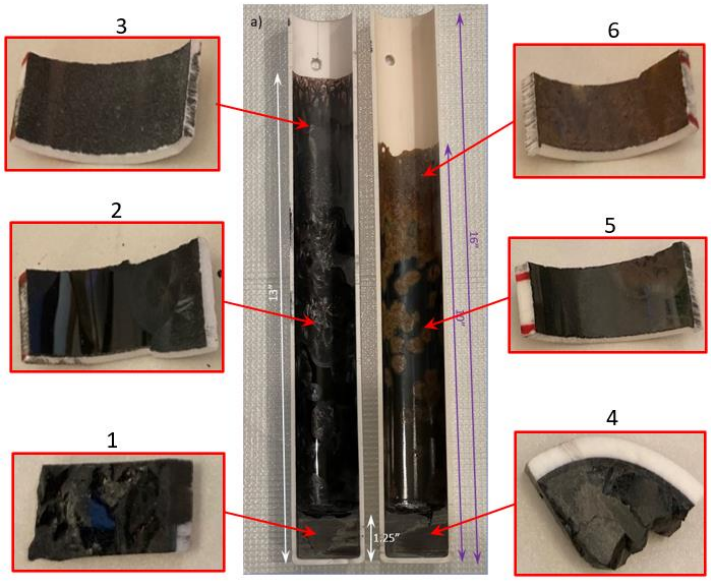

Figure 8. Samples of JSC 1A lunar regolith simulant melts extracted along the two tubular crucibles shown in Figure 5 to be analyzed via SEM/EDX.

The SEM/EDX composition analysis on samples 1, 2, and 3 depicted in Figure 8 are listed in Table 1, the composition of JSC 1A lunar regolith simulant reported in the literature[8] is posted in the first column of Table 1 to have a comparative baseline. The composition on the bottom (sample 1) is basically like the one reported in the literature[8]; the composition of iron (Fe), magnesium

(Mg) and phosphorus (P) are substantially reduced as the melt moved upwards from the bottom (sample 1) passing by the middle (sample 2), and ending at the top (sample 3). Fe composition starts at 8.39% (8.35% in the literature) on the bottom (sample 1) decreasing to 5.27% at the middle (sample 2) and keeps reducing even further to 1.91% at the top (sample 3). Mg experienced a decrement from 5.25% (5.25% in the literature) up to 0.53% at the top (sample 3). The decrement of these and other elements (such as Na, and P) due to decomposition/segregation of their respective native oxides leads to the increment of other components that did not experience decomposition; Aluminum (Al) concentration increases from 8.4% (9.34% in the literature).

Wt %	Literature	Sample 1 Bulk	Sample 2 Bulk	Sample 3 Bulk
O	44.02	44.06 ± 2.14	45.86 ± 0.72	47.47 ± 1.01
Si	22.04	21.54 ± 0.97	19.97 ± 0.39	21.48 ± 0.37
Ti	1.04	0.97 ± 0.10	0.86 ± 0.06	0.43 ± 0.17
Al	8.44	9.34 ±0.52	14.17 ± 0.33	16.75 ± 0.59
Fe	8.35	8.39 ±1.35	5.27 ± 0.43	1.91 ± 0.89
Mg	5.72	5.25 ± 0.22	2.95 ± 0.03	0.53 ± 0.21
Ca	7.15	7.19 ± 0.63	7.00 ± 0.30	9.53 ± 0.69
Na	2.12	2.24 ± 0.13	1.99 ± 0.02	1.64 ± 0.20
K	0.65	0.64 ± 0.05	0.66 ± 0.08	0.15 ± 0.05
Mn	0.15	0.15 ±0.05	0.10 ± 0.06	0.07 ± 0.05
Cr	0.01	0.05 ± 0.03	0.04 ± 0.01	0.05 ± 0.04
P	0.31	0.28 ± 0.03	0.36 ± 0.04	0.04 ± 0.03

Table 1. SEM/EDX composition analysis of samples 4, 5, and 6 obtained at 1,400 Celsius and 1.2E-3 torr.

The SEM/EDX composition of samples 4, 5, and 6 generated at 1,400 Celsius and 1.2E-3 torr located in the bottom, middle, and top respectively of the tubular crucible are listed in Table 2. Formation of dendrites due to fractional segregation coupled with decomposition was evident in samples 5 and 6 (middle and top locations). Figure 9a and 9b show the SEM/EDX images of the dendrites spotted in samples 5 and 6 respectively; the white areas in Figure 9b happened to be tungsten (W) coming from the wire installed to hang the alumina insulation blocks on top of the tubular crucible. The composition of the dendrites is included in Table 2, samples 5 and 6 have two columns each to include the composition on the dendrites. Fe composition also decreases, from 7.85% to 4.03% but in the dendrite is enriched on the top (sample 6) reaching 12.9%. The same pattern happened to Mg, it increased in the bulk from 5.36% to 1.68% but enriched in the dendrite reaching 6.75%. P composition, the element that also significally increased along with Fe and Mg in the first case, also decreased from 0.29% on the bottom to 0.12% on the top but it enriched in the dendrite reaching 0.44%. Silicon, the second abundant element in the JSC 1A lunar regolith simulant is depleted in the dendrite, from 21.67% in the bulk to 17.98% in the dendrite.

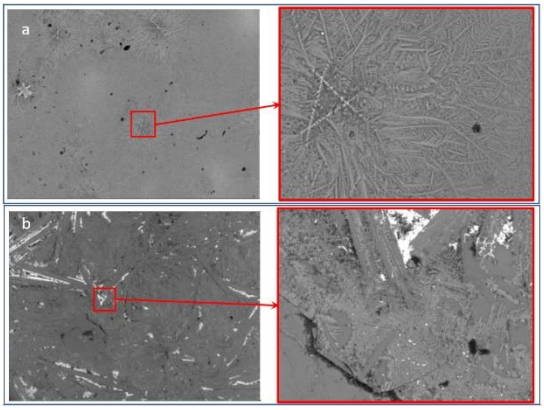

Figure 9. SEM images of segregated dendrites formation on samples 5 (a) and 6 (b) respectively.

			Sample 5		Sample 6	
Wt %	Literature	Sample 4 Bulk	Bulk	Dendrites	Bulk	Dendrites
O	44.02	44.74 ± 1.83	42.94 ± 0.71	41.60 ± 1.15	44.13 ± 9.35	47.21 ± 15.12
Si	22.04	21.67 ± 0.57	18.65 ± 0.12	14.84 ± 5.11	19.98 ± 4.33	17.98 ± 8.53
Ti	1.04	0.95 ± 0.08	0.95 ± 0.05	0.78 ± 0.29	0.59 ± 0.31	2.00 ± 0.85
Al	8.44	8.89 ± 0.53	11.91 ± 0.25	13.57 ± 3.96	15.24 ± 3.36	14.78 ± 4.06
Fe	8.35	7.85 ± 0.84	9.83 ± 0.37	12.98 ± 3.94	4.03 ± 2.62	12.90 ± 6.07
Mg	5.72	5.36 ± 0.19	5.60 ± 0.15	6.77 ± 2.83	1.68 ± 1.5	6.75 ± 2.43
Ca	7.15	7.04 ± 0.51	7.07 ± 0.45	7.31 ± 2.99	7.83 ± 2.08	3.42 ± 1.37
Na	2.12	2.35 ± 0.15	1.94 ± 0.15	1.26 ± 0.40	2.10 ± 0.53	2.69 ± 1.60
K	0.65	0.68 ± 0.06	0.69 ± 0.02	0.40 ± 0.14	0.2 ± 0.09	0.82 ± 0.66
Mn	0.15	0.14 ± 0.05	0.19 ± 0.07	0.19 ± 0.03	0.10 ± 0.09	0.31 ± 0.17
Cr	0.01	0.06 ± 0.03	0.04 ± 0.01	0.16 ± 0.17	0.04 ± 0.03	0.35 ± 0.67
P	0.31	0.29 ± 0.03	0.23 ± 0.01	0.16 ± 0.05	0.12 ± 0.05	0.44 ± 0.30

Table 2. SEM/EDX composition analysis of samples 4, 5, and 6 obtained at 1,400 Celsius and 1.2E-3 torr.

VI. Summary

Thermal Marangoni effect alone and coupled with fractional decomposition of metal oxides releasing O_2 have been corroborated on molten JSC-1A lunar regolith simulant through long upwards migration paths, 10 and 13 inches respectively validating further the proposed approach for extraterrestrial mining. These two coupled phenomena, thermal Marangoni effect and fractional decomposition, will be more prominent on extraterrestrial surfaces under much higher vacuum and reduced gravity.

The test stand designed and built by the authors can operate at temperatures as high as 1,600 Celsius and house longer and wider tubular crucibles to carry larger samples with lengthier self-transportation path. The comprehensive 3D model built by the authors demonstrated to be a crucial tool to determine the optimal location of the tubular crucible to obtain the largest temperature gradient along the crucible's wall to boost the thermal Marangoni effect. SEM/EDX analysis were conducted on melt samples along the upwards migration path to quantify and corroborate the fractional decomposition and segregation of the melt.

Self-transportation, due to Marangoni effect, without fractional decomposition that would be required in the non-mechanical extraterrestrial mining approach was witnessed along 13 inches in the first case. Additionally, self-transportation coupled with fractional decomposition/segregation of the melt at higher temperature that would be required for sustainable extraction/refinery and all-in-one extraterrestrial mining approach was also witnessed (and quantified via SEM/EDX analysis) along 10 inches in the second case.

This novel approach might be an alternative to pursue sustainable environmental-friendly production of metals, such as aluminum that generates more CO_2 by weight than aluminum.

References

[1] Dominguez J. A., Whitlow J., Marangoni effect and its potential utilization in supporting lunar habitats and other extraterrestrial endeavors, Advances in Space Research 69 (2022) 2259–2267.

[2] Scriven, L. E.; Sterling, C. V. Nature 1960, 187, 186–188.

[3] Fanton, X.; Cazabat, A. M. Langmuir 1998, 14, 2554–2561.

[4] Levich, V. G. Physicochemical Hydrodynamics; Prentice-Hall international Series in the Physical and Chemical Engineering Sciences: Englewood Cliffs, NJ, 1962; pp 384–390.

[5] Fournier, J. B.; Cazabat, A. M. Europhysics Letters 1992, 20, 517–522.

[6] Tazioukov F., Garifoullin F., Norden P., Ossipov P., Karibullina F., (1996), Surface Migration of Oil in Vacuum Systems, Vakuurn in Forschung und Praxis, vol. 8, issue 2. pp. 105-108.

[7] Kundan, A., Plawsky, J.L., Wayner, P.C., Chao, D.F., Sicker, R.J., Motil, B.J., Lorik, T., Chestney, L., Eustace, J., Zoldak, J., 2015. Thermocapillary Phenomena and Performance Limitations of a Wickless Heat Pipe in Microgravity. Physical Review Letters PRL 114 146105.

[8] Gustafson, R. JSC-1A Lunar Regolith Simulant Availability and Characterization, NASA Marshall Space Flight Center workshop, slide 6. https://www.nasa.gov/sites/default/files/atoms/files/03_jsc-1a_lunar_regsimulant_update_bgustafson.pdf